

Modelling of viscoelasticity of thermoplastic polymers in micro hot embossing process

F. Rabhi¹, G. Cheng², T. Barriere¹

¹ Université de Franche-Comté, SUPMICROTECH, CNRS, institut FEMTO-ST, F-25000
Besançon, France

² INSA CVL, Université Tours, Université Orléans, LaMé, 3 rue de la Chocolaterie, CS
23410, 41034 Blois Cedex, France

Abstract

The fabrication of micro-scale components requires a high degree of precision in the manufacturing process. The microsystems obtained by using the hot embossing (HE) process is widely developed in various fields, since it allows to emboss complex structures at micro/nano scale such as optical sensors, diffractive lenses, microfluidic channels and so on. The development of micro-parts via this process requires in-depth analysis of the surface quality obtained and the mould filling rate. It is essential to analyze the influence of the properties of the polymers employed in the HE process on the final filling quality of the mould, in order to optimize the process in terms of cost, quality and productivity. In this research, compression tests were carried out with two polymers, Poly(methyl methacrylate) (PMMA) and Polycarbonate (PC), at different temperatures ($T_g+20^\circ\text{C}$ and $T_g+30^\circ\text{C}$) to determine their elastic, plastic and viscous properties. Numerical simulation of the HE process was carried out by using Abaqus finite element software, taking into account the mechanical properties of both polymers and the characteristics of microchannels. The aim was to analyze the effect of the elastoviscoplastic properties of the materials on the mould filling rate at different temperatures. The two-layer viscoplastic model was employed to describe the viscous behavior of the polymers on mould filling. Numerical simulation of HE process with PMMA shows that the mould cavity is completely filled with elastoviscoplastic behaviors, and the filling rate increases as a function of mould displacement. On the other hand, for PC, the viscous properties have little influence on the filling of the mould, and good filling of the cavity is obtained with the elastoplastic property.

Keywords: Hot embossing, Two-layer viscoplastic model, Numerical simulation

1. Introduction

The demand for microstructures continues to grow. It needs to improve the manufacturing process for fabricating the micro components at lower cost and in less time. Hot embossing (HE) is the perfect technique for manufacturing small-scale devices on a large scale. Thermoplastic polymers such as PS, PMMA and PC are mainly used as processing materials in HE [1]. HE is a promising technology for mass production of PMMA and PC microstructures due to its high efficiency, low cost, and high replication accuracy.

Cheng *et al.* [2] successfully employed HE with an innovative injection-moulding press and mould to manufacture PMMA microfluidic systems slightly above its T_g . Wang *et al.* [3] took into account the polymer's recovery properties and optimized the related processing duration and temperature of the micro HE process and achieved a filling with high precision and efficiency. Kasztelanic *et al.* [4] employed HE process to develop the optical devices with ZBLAN glass. Their work was aimed at optimizing the process to eliminate the product defects. Deshmukh *et al.* [5] analyzed the replication accuracy of embossed micro-channel by optimizing the HE processing parameters. The process was also numerically simulated by using different methods to analyze the quality of the product obtained. Worgull *et al.* [6] employed Moldflow to simulate mould filling, and applied ANSYS for demoulding simulation to describe the typical damage of the replicated microstructures obtained by HE process.

Many experimental tests have been performed to analyze the behaviour of amorphous thermoplastic polymers and identify their properties in the temperature range below T_g . Cheng *et al.* [7] employed the compression tests to investigate the viscoelastic behaviour of PMMA during the micro HE process. The viscoelastic, viscoplastic, and elastic-viscoplastic models have been developed to explore the physical constitutive behaviour laws of amorphous thermoplastic polymers. The **Two-Layer Visco-Plastic** (TLVP) model behaviour law was initially developed for metals. It was composed by two parallel elastoplastic and viscoelastic branches. Charkaluk *et al.* [8] employed an elastic-viscoplastic constitutive law with a two-layer model under thermo-mechanical loading for cast-iron exhaust manifolds. Abdel-Wahab *et al.* [9] investigated the plastic, elastic and viscous properties of PMMA at large strains with a TLVP

model. The parameters were identified according to the experimental data from different mechanical tests under various loading conditions below T_g .

In this paper, the HE process for producing microchannels in PMMA and PC was investigated numerically with the TLVP model. Compression tests were carried out at $T_g+20^\circ\text{C}$ and $T_g+30^\circ\text{C}$ to identify the elastic, plastic and viscous parameters of the two polymers. HE simulation was carried out to determine the influence of material parameters on mould filling efficiency.

2. Description of HE process and TLVP model

2.1. Description of micro HE process

The HE process is one of the polymer replication processes for elaborating the microstructures. The process is especially suited for manufacturing small and medium series of microcomponents [10]. Fig. 1 shows the steps of HE process to elaborate micro-scale components (Moulding, cooling, demoulding). As illustrated in Figure 1, the process consisted of a mould, which was pressed against a polymer substrate that was heated to a temperature that was typically above the glass transition temperature of the polymer material. A holding time was necessary under heat and pressure to allow the polymer to flow completely all the patterns in the mould. Upon cooling down and separation (demoulding step) of the mould from the polymer substrate, a reversed image of the pattern would be imprinted on the polymer surface [11].

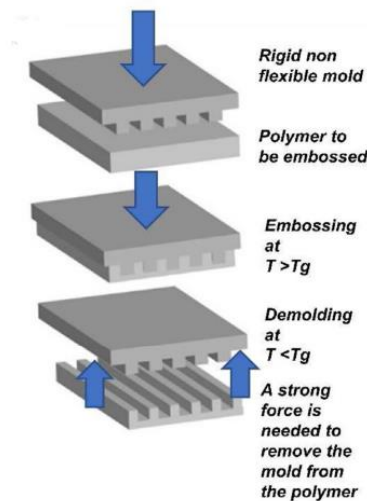


Fig. 1. Schematic picture of the HE technique [12].

The main advantage of HE is the possibility to manufacture the devices with various patterns thanks to its easy operation, high accuracy, mass production, short cycle time and cost effective. The HE is employed to produce different geometries in microscales [Fig. 2](#). HE process can be used to replicate the geometries from simple (triangular, rectangular with shape repetition...) to complex shapes (microfluidic, MEMS...).

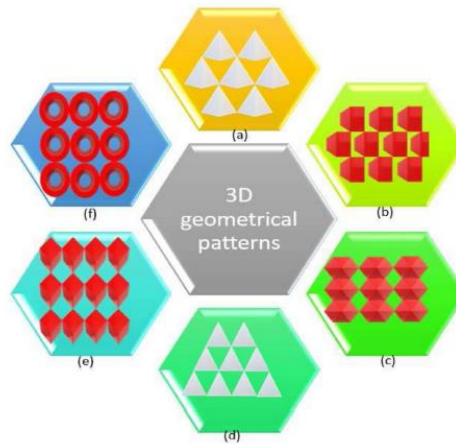


Fig. 2. Different types of 3D geometrical patterns [13].

2.2. Description of TLVP model

This model was employed to describe the viscous and plastic behaviours of polymers at high temperature. In this research, the model was adapted to describe the behaviour of PMMA and PC. All the parameters of TLVP were identified based on the compression tests. The TLVP model is shown in [Fig. 3](#).

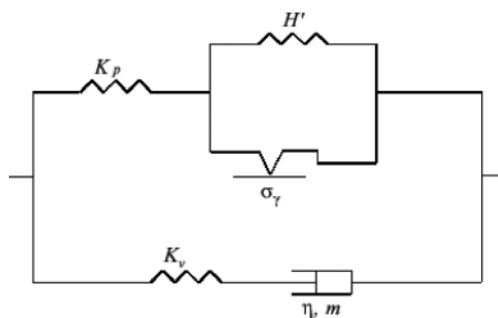


Fig. 3. One-dimensional idealisation of the TLVP model [14].

The TLVP model considers the elastic, plastic, and viscous deformations of a material and was implemented in the Abaqus® software. The elasticity is defined by the

linear isotropic elastic part. f is the proportion of elasticity in the viscoelastic branch to the total elasticity. The total modulus is defined as $K = K_p + K_v$. f is defined as follows:

$$\begin{cases} f = \frac{K_v}{K_p + K_v} \\ K_v = K - K_p \\ f = \frac{K - K_p}{K} \end{cases} \quad (1)$$

where K_p the elastic modulus of the elastoplastic branch and K_v is the elastic modulus of the viscoelastic branch.

The total stress is defined by adding the viscous stress σ_v in the viscoelastic branch and stress σ_p in the elastoplastic branch and the total stress σ is given by:

$$\sigma = \sigma_p + \sigma_v \quad (2)$$

A time-hardening power law was used for the viscous behaviour by setting $m = 0$; this means that the viscous strain rate $\dot{\varepsilon}$ is independent of time:

$$\sigma_v = A \frac{1}{n} \dot{\varepsilon}^n \quad (3)$$

$$\dot{\varepsilon} = A \sigma_v^n t^m \quad (4)$$

where A and n represent the Norton–Hoff law, t represents the testing time.

The elastic strain ε^{el} is divided into a viscoelastic part ε_v^{el} and elastoplastic part ε_p^{el} :

$$\varepsilon^{el} = f \varepsilon_v^{el} + (1 - f) \varepsilon_p^{el} \quad (5)$$

The total strain includes the elastic and plastic strains in the elastoplastic branch ε^{pl} and the viscous strain in the viscoelastic branch ε^v :

$$\varepsilon = \varepsilon^{el} + f \varepsilon^v + (1 - f) \varepsilon^{pl} \quad (6)$$

3. Results of experimental characterization tests

Uniaxial compression tests were performed to identify the material parameters of the viscoplastic constitutive behaviour at $T_g+20^\circ\text{C}$ and $T_g+30^\circ\text{C}$ for PMMA and PC. The plastic parameters of the polymers are extracted in the plastic domain of the stress-strain curves. According to the stress-strain curve of the compression response at T_g+20

$^{\circ}\text{C}$ and $T_g+30^{\circ}\text{C}$, the plastic strains were identified at various stresses, as listed in [Table 1](#).

Table 1. Plastic strain parameters of PMMA at $T_g + 20^{\circ}\text{C}$ and $T_g+30^{\circ}\text{C}$

	$T_g+20^{\circ}\text{C}$		$T_g+30^{\circ}\text{C}$	
	σ^p (MPa)	ε^p	σ^p (MPa)	ε^p
PMMA	0.50	0	0	0
	0.51	0.01	0.10	0.01
	0.90	0.04	0.30	0.05
	1.49	0.11	0.5	0.11
PC	0.20	0	0	0
	0.39	0.40	0.14	0.40
	0.62	0.50	0.21	0.50
	0.90	0.56		

The parameter f was calculated with [Eq. \(1\)](#) and the material constants in the elastic-viscoplastic model were summarised in [Table 2](#).

Table 2. TLVP model parameters at $T_g + 20^{\circ}\text{C}$.

Parameters	PMMA	PC
K_p (MPa)	3.61	2.17
K (MPa)	33.38	31.73
f	0.89	0.93
A (Pa)	6.63×10^{-6}	1.71×10^{-4}
n	0.88	0.70
m	0	0

4. Results of numerical simulation of HE process

The numerical simulation of the HE process was carried out on Abaqus by taking into account the elastic, plastic and viscous properties of PMMA and PC at different temperatures. A 2D axisymmetric geometry model representing the mould and polymer is illustrated in [Figure 4](#). The filling efficiency was investigated with different displacement of the mould : $d=0.05$ mm, $d=0.10$ mm, $d=0.15$ mm and $d=0.20$ mm.

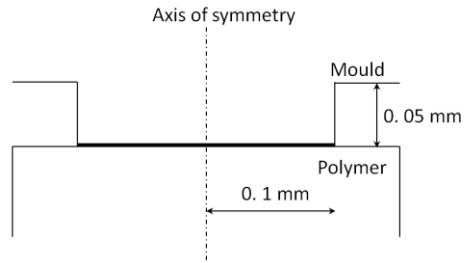


Fig. 4. 2D axisymmetric geometry model used to simulate the micro HE process.

4.1. Results and discussions of mould filling ratio for PMMA

Numerical simulation was carried out for both polymers in order to determine the Von-Mises stresses as well as to determine the influences of the material properties on the mould filling rate.

The results of the numerical simulation of the HE process for PMMA at $T_g+20^\circ\text{C}$ in terms of mould filling rate are shown in [Figure 5](#). The filling rate increases with mould displacement. Elastic, elastoplastic and elastic-viscoplastic behaviours are considered in the numerical simulation. The mould is 99.99% filled by Applying the elastovisco-plastic behaviour on PMMA. It indicates that the viscous behaviour plays a very important role in the filling of micro cavity.

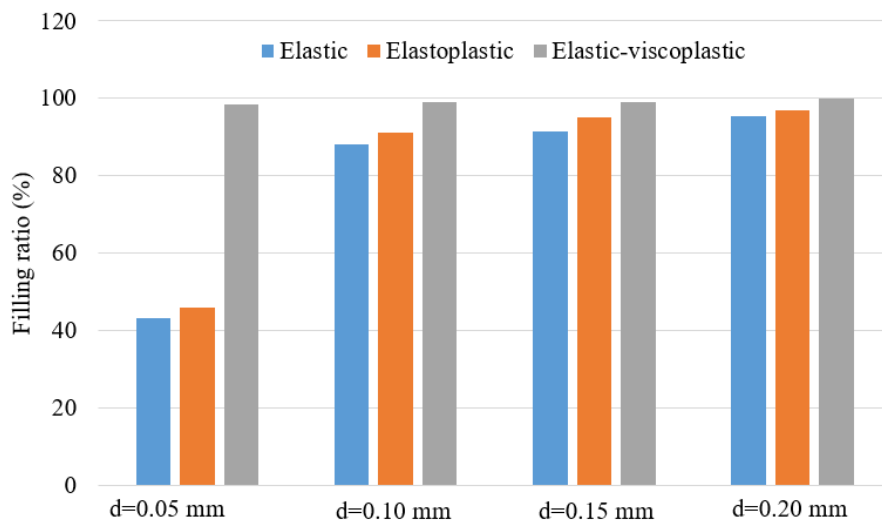


Fig. 5. Cavity filling ratio versus different imposed displacements and constitutive behaviours.

The [Figure 6](#) shows the filling of the mould with the combination of PMMA's elastic, plastic and viscous properties at $T_g+20^\circ\text{C}$. The cavity filling ratio increased with the imposed displacement. When the imposed displacement was 0.2 mm, the micro-cavity was almost completely filled. Based on the filling ratios obtained at the same imposed displacement of 0.2 mm, using the elastic-viscoplastic model increased the filling ratio in the numerical simulation. This result demonstrates that the micro-cavity was almost completely filled when the elastic, plastic, and viscous behaviours were all considered during the simulation.

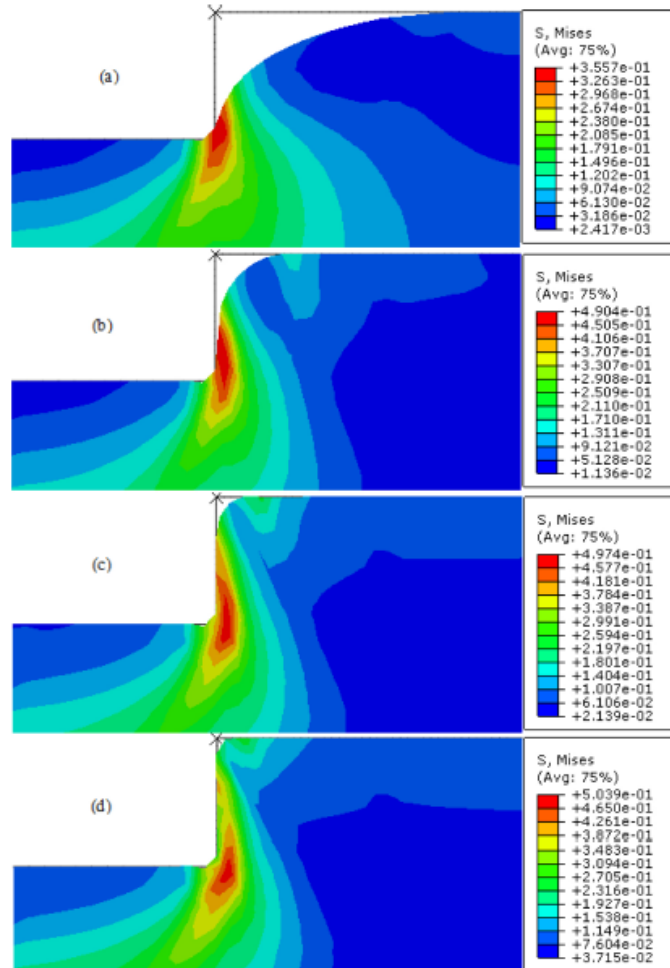


Fig. 6. Von Mises stress results for the PMMA substrate specimen during the whole process with the elastic-viscoplastic model at $T_g+20\text{ }^\circ\text{C}$: (a) $d = 0.05\text{ mm}$, (b) $d = 0.1\text{ mm}$, (c) $d = 0.15\text{ mm}$, and (d) $d = 0.2\text{ mm}$.

4.2. Results and discussions of mould filling ratio for PC

Numerical simulation of the HE process was also carried out at $T_g+20\text{ }^\circ\text{C}$ and $T_g+30\text{ }^\circ\text{C}$ for PC, taking into account the elasto-viscoplastic parameters of the polymer. The filling rate in the elasto-viscoplastic case was similar to that in the case where we only used the elastoplastic properties of PC. This means that for PC, the viscous properties have less influence on the mould filling rate.

In order to visualize the influence of temperature on the mould fill rate, the [Figure 7](#) shows a comparison of filling rates for PC as a function of temperature ($T_g+20^\circ\text{C}$ and $T_g+30^\circ\text{C}$) and mould displacement, taking into account elastic and elastoplastic properties. The filling ratio increases slightly with temperature.

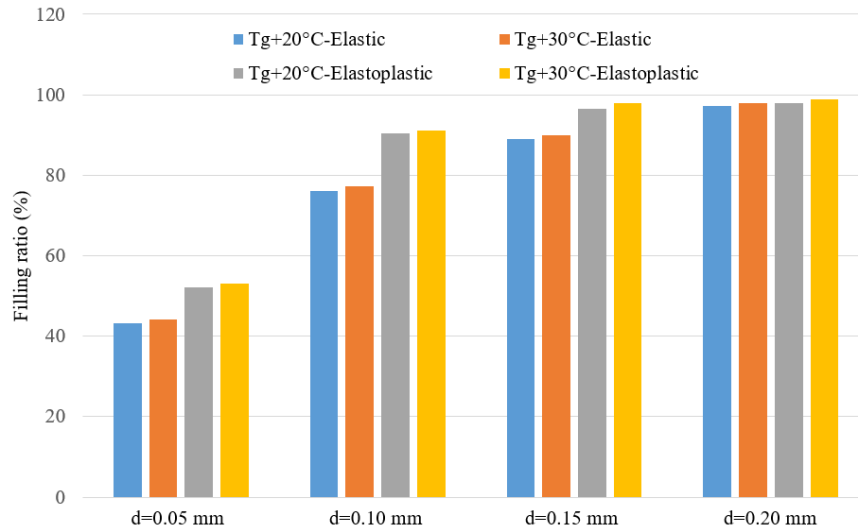


Fig. 7. Cavity filling ratio versus different imposed displacements for PC with elastic and elastoplastic behaviours.

5. Conclusions

The aim of this work was to investigate the influence of the elastic, elastoplastic, and elastic viscoplastic behaviours of polymers (PMMA and PC), on the filling efficiency of the micro HE process. The TLVP model was employed to model the elasto-viscoplastic property. The identification of the elastic, plastic and viscous parameters was effectuated according to the true stress–true strain curves obtained in uniaxial compression tests at different temperatures: $T_g+20^\circ\text{C}$ and $T_g+30^\circ\text{C}$.

For PMMA, a filling rate of 99% was obtained taking into account the elasto-viscoplastic property, which means that the viscous property of PMMA influences the filling rate. For the PC, the viscous property possesses less influence on the filling rate of the mould in HE process.

References

- [1] G. Cheng, M. Sahli, J.C. Gelin, T. Barrière. Physical Modelling, Numerical Simulation and Experimental Investigation of Microfluidic Devices with Amorphous Thermoplastic Polymers Using a Hot Embossing Process. *Journal of Materials Processing Technology*, 229; 36–53; 2016. <https://doi.org/10.1016/j.jmatprotec.2015.08.027>.
- [2] Cheng G, Sahli M, Gelin JC, Barrière T. Process parameter effects on dimensional accuracy of a hot embossing process for polymer-based micro-fluidic device manufacturing. *Int. J. Adv. Manuf. Technol.* 75:225–235; 2014. <https://doi.org/10.1007/s00170-014-6135-6>.
- [3] Wang J, Yi P, Deng Y, Peng L, Lai X, Ni J. Recovery behavior of thermoplastic polymers in micro hot embossing process. *J. Mater. Process. Technol.* 243:205–216; 2017. <https://dx.doi.org/10.1016/j.jmatprotec.2016.12.024>
- [4] Kasztelanica R., Cimek J., Kujawa I., Golebiewski P., Filipkowski A., Stepień R., Sobczak G., Krzyżak K., Pięrciński K., Buczyński R.. Mid-infrared ZBLAN glass optical components made by hot embossing technique. *Optics and Laser Technology* 157; 108655; 2023. <https://doi.org/10.1016/j.optlastec.2022.108655>.
- [5] Deshmukh S.S., Kar T., Som S., Goswami A.. Investigation of replication accuracy of embossed micro-channel through hot embossing using laser patterned copper mold. 60; 2222-2229; 2022. <https://doi.org/10.1016/j.matpr.2022.03.128>.
- [6] Worgull M., Hecke M.. New aspects of simulation in hot embossing. *Micro-syst. Technol.* 10; 432–437; 2004. <https://doi.org/10.1007/s00542-004-0418-z>.
- [7] G. Cheng, M. Sahli, J.C. Gelin, T. Barrière. Physical modelling, numerical simulation and experimental investigation of microfluidic devices with amorphous thermoplastic polymers using a hot embossing process. *J. Mater. Process. Technol.*; 229:36–53; 2016. <https://doi.org/10.1016/j.jmatprotec.2015.08.027>.
- [8] E. Charkaluk, A. Bignonnet, A. Constantinescu, K. Dang Van. Fatigue design of structures under thermomechanical loadings. *Fatigue Fract. Eng. Mater. Struct.* 25; 1199–1206; 2002. <https://doi.org/10.1046/j.1460-2695.2002.00612.x>
- [9] AA. Abdel-Wahab, S. Ataya, VV. Silberschmidt. Temperature-dependent mechanical behaviour of PMMA: Experimental analysis and modelling. *Polym. Test.* 58:86–95; 2017. <https://doi.org/10.1016/j.polymertesting.2016.12.016>

[10] M. Worgull, J.F. Héту, K.K. Kabanemi, M. Hecke. Modeling and optimization of the hot embossing process for micro- and nanocomponent fabrication. *Microsystem Technologies* volume 12; 947–952; 2006. DOI [10.1007/s00542-006-0124-0](https://doi.org/10.1007/s00542-006-0124-0).

[11] S. H. Ng & Z. F. Wang & R. T. Tjeung & N. F. de Rooij. Development of a multi-layer microelectrofluidic platform. *Microsystem Technologies* 13; 1509-1515; 2007. [10.1007/s00542-006-0341-6](https://doi.org/10.1007/s00542-006-0341-6).

[12] D.R. Barbero, M.S.M. Saifullah, P. Hoffmann, H.J. Mathieu, D. Anderson, G.A.C. Jones, M.E. Weiland, U. Steiner, Facile preparation of superhydrophobic PVDF microporous membranes with excellent anti-fouling ability for vacuum membrane distillation, *Adv. Funct. Mater.* 17 (2007) 2419e2425, <https://doi.org/10.1002/adfm.200600710>.

[13] Jaishree, A. Bhandari, N. Khatri, Y.K. Mishra, M.S. Goyat. Superhydrophobic coatings by the hot embossing approach: recent developments and state-of-art applications. *Materials Today Chemistry* 30; 101553; 2023. <https://doi.org/10.1016/j.mtchem.2023.101553>.

[14] Rabhi F., Cheng G., Barriere T., Hocine N. A.. Influence of elastic-viscoplastic behaviour on the filling efficiency of amorphous thermoplastic polymer during the micro hot embossing process. *Journal of Manufacturing Processes*, 59 ; 487-499 ; 2020. <https://doi.org/10.1016/j.jmapro.2020.09.032>.